Title

Application of quantitative computed tomography for assessment of trabecular bone mineral density, microarchitecture and mechanical property

Journal

Clinical Imaging, 40(2)

ISSN

0899-7071

Authors

Mao, Song Shou
Li, Dong
Luo, Yanting
et al.

Publication Date

2016-03-01

DOI

10.1016/j.clinimag.2015.09.016

Peer reviewed

Clinical Imaging xxx (2015) xxx–xxx

Contents lists available at ScienceDirect

Clinical Imaging

journal homepage: http://www.clinicalimaging.org

Application of quantitative computed tomography for assessment of trabecular bone mineral density, microarchitecture and mechanical property

Song Shou Mao, Dong Li, Yanting Luo, Younus Saleem Syed, Matthew J. Budoff*

Los Angeles Biomedical Research Institute at Harbor-UCLA, 1124 West Carson Street, Torrance, CA 90502

ARTICLE INFO

Article history:
Received 1 April 2015
Received in revised form 17 July 2015
Accepted 10 September 2015
Available online xxxx

Keywords:
Quantitative CT
Multi-row detector CT
Bone mineral density
Calibration phantom

ABSTRACT

Osteoporosis is a common metabolic bone disease, causing increased skeletal fragility characterized by a low bone mass and trabecular microarchitectural deterioration. Assessment of the bone mineral density (BMD) is the primary determinant of skeletal fragility. Computed tomography (CT)-based trabecular microarchitectural and mechanical assessments are important methods to evaluate the skeletal strength. In this review, we focus the feasibility of QCT BMD measurement using a calibration phantom or phantomless. The application of QCT could extend the bone mineral density assessment to all patients who underwent a heart, lung, whole-body, and as well as all routine clinical implications of CT scan.

1. Introduction

Fragility fracture is a common public health problem with a high mortality, morbidity and cost. Osteoporosis significantly related to bone fragility and consequent fracture. Therefore, the diagnosis and monitoring of osteoporosis with BMD measurement are strongly associated with bone health. BMD explains about 70–75% of the variance in strength [1,2]. The World Health Organization (WHO) proposed guidelines for the diagnosis of osteoporosis based on BMD measurement by using dual X-ray absorptiometry (DXA) in 1994 [3]. Since then, DXA has been widely used for the epidemiological studies, clinical research and treatment strategies of osteoporosis [4,5]. Lumbar QCT had been employed in the 1980s [6], is also recommended as an acceptable method in the diagnosing osteoporosis by the WHO. A certain number of new technologies have been developed for assessing bone mineral density until now, including peripheral QCT (pQCT) [7], μCT (microCT) [8], magnetic resonance imaging (MRI) [9,10] and quantitative ultrasound (QUS) [11]. Compared to DXA, QCT offers superior sensitivity in diagnosing osteoporosis, monitoring the bone density changes, and evaluating the bone trabecular microarchitectural and mechanical property simultaneously, but still considered a supplemental method due to its high radiation [12]. Two-dimensional QCT BMD measurement of the spine tended to show a lower precision, which lead to limited employment [13]. In the U.S., there are over 12,000 multidetector CT (MDCT) scanners [14]. CT scanning is widely used in diagnosis and prognosis for lung cancer, cardiac disease, as well as abdominal and pelvic disease. With the high resolution MDCT images, clinicians can obtain important information of BMD, trabecular microarchitectural and mechanical property, as an additional utility to clinical applications. The aims of the review are to evaluate: 1. Method and feasibility of QCT in BMD assessment with the use of phantom or phantomless calibration, 2. The ability of QCT to diagnose the osteoporosis and to monitor the aging-, disease- and medicine-related BMD changes, 3. Feasibility in the trabecular microarchitectural and mechanical assessment using current MDCT images.

2. Method of QCT bone mineral density measurement

2.1. QCT technique in the lumbar spine

Hounsfield unit (CTHU)-based QCT technique has been utilized over the last three decades [3,6]. Lumbar QCT was the only method initially [6]. With this technique, the CT image was obtained using routine scan parameters in the lumbar spine with a calibration phantom under the patient's back. Lower radiation dose protocol was used in most studies, such as 80kVp/140 mAs or 140 kVp/80 mAs with 5 mm image thickness or greater [6,15]. The calibration phantom technique has two functions, translating the CTHU to the bone units (mg/mm^3) and calibrating CTHU within location, patients and scanners made by many manufacturers. The calibration standard was originally designed by Cann et al [6] (Mindway, South San Francisco, CA, USA). Subsequently, two standard phantoms were also used commonly, developed by the

Abbreviations: MDCT, Multi-row detector CT; CACs, Coronary artery calcium scan; QCT, Quantitative CT; BMD, Bone mineral density; CTHU, CT hounsfeild unit.

* Corresponding author. Los Angeles Biomedical Research Institute at Harbor-UCLA, 1124 West Carson Street, Torrance, CA 90502. Tel.: +1 310 222 4107; fax: +1 310 782 9652.
E-mail addresses: smao@labiomed.org (S.S. Mao), dli@labiomed.org (D. Li), yluo@labiomed.org (Y. Luo), ysyed@labiomed.org (Y.S. Syed), mbudoff@labiomed.org (M.J. Budoff).

http://dx.doi.org/10.1016/j.clinimag.2015.09.016
0899-7071/

Image analysis, (Columbia, KY, USA) [16] and Siemens Medical System [17] (Erlangen, Germany). Those phantoms consist of a water-equivalent solid resin matrix and rods filled by a calcium material with varying concentration. The calcium material usually includes a dipotassium hydrogen phosphate or calcium hydroxyapatite (CaHA). The concentrations of the calcium material in rods are equivalent to 200, 100, 50, 0 mg/mm^3 and larger than 200 mg/mm^3 or close the density of fatty tissue [6,16]. The lumbar trabecular bone and the phantom rods at the center area (L1–L4, or L1–L3) can be segmented semi-automatically by a computer system. The trabecular BMD, as well as the T and Z score can be calculated automatically by using the conversion equations and their standard references developed by the manufacturers. Those references included mean values and standard deviation in the younger group and every age group (most from 20 to 85 years) of men and women.

To date, manufacturers have not developed a uniform standard reference for calculating the T score with CT. Theoretically, T-scores derived by QCT should not be used to assign a diagnostic category, as it may differ from that of DXA [18]. Nonetheless, the standard of osteoporosis based on T score by DXA was used in most QCT studies [19–22]. The American College of Radiology (ACR) has published guidelines for the performance of QCT in lumbar spine in 2008 and amended in 2014. Based on the guidelines, volumetric trabecular BMD values from 120 to 80 mg/cm^3 were defined as osteopenic and below 80 mg/cm^3 as osteoporosis [18]. This definition was suggested to assigned as a diagnostic criteria approximately equivalent to WHO diagnostic categories with a hip DXA. In an analysis of osteoporosis diagnosis in 2028 lumbar QCT data [23], the number of individuals detected with osteoporosis (<80 mg/cm^3, and T<-2.5) was 74 and 379 in 1011 women, 74 and 191 in 1017 men by ACR and Image analysis programs respectively. The result demonstrated a significant difference in the reference value for the diagnosis of osteoporosis between ACR and Image analysis methods. Therefore, validating and establishing a uniform standard reference is an important work for future BMD assessment.

2.2. Thoracic vertebral QCT with a routine heart scan (Fig. 1)

Osteoporosis and coronary atherosclerosis have been recognized as co-existing conditions with aging, and both may share common etiologies and pathogenesis [24,25]. They are independent risk factors for bone fracture and cardiovascular disease, consequently, resulting in significant medical and financial cost each year. In the United States alone, osteoporosis affects more than 25 million men and women, 1 in 2 women and 1 in 5 men aged 50 and above during their lifetimes [26]; meanwhile coronary artery calcium burden (CAC), as a specific marker of atherosclerosis was noted in 50–70% in men and 35–45% in women older than 45 years in multi-ethnic populations [27]. The diagnosis of osteoporosis and coronary atherosclerosis is important in the prevention, prediction and management of bone fracture and coronary artery disease. In women, menopause is associated with increased bone loss and deleterious changes in the physiological bone structure. BMD examination was recommended as a screening to determine skeletal status in men aged 65 years or older [28]. Women who have experienced menopause and men who have the risk of fracture before the age of 65 must also be considered for BMD screening [28,29]. In general, there is a growing consensus that subjects aged ≥50 years should be evaluated for osteoporosis [30].

Compared to the CAC CT scan, QCT has not been used extensively as a common technique for bone mineral measurement due to its high radiation (3.5 mSv) [31] and cost. If the thoracic trabecular BMD can be measured from the same cardiac CT image with only one mSv radiation, it should potentially cover most populations recommended for BMD screening. Furthermore, the deformity at mid-lower thoracic spine can be evaluated simultaneously, which is a common anatomic site of fracture (most fractures present in T7, T12 and L1) [32]. The validated studies have demonstrated that the EKG-gated heart CT scans with a calibration phantom can be used to assess the thoracic vertebrae BMD using the lumbar QCT technique [21,33,34]. The reference value for the standardization of the T and Z score in the thoracic vertebrae BMD had been developed [21].

In current CAC scanning protocols, three thoracic spines can be evaluated in all studies at least. Since the variation exists within individual spinal BMD [35], fixing the levels is an important issue for decreasing the precision error of BMD assessment. The continuous three thoracic spines (3 T) beginning from the level of the left coronary artery are commonly used to assess the trabecular BMD on CAC scanning [21,36]. A similar segmenting and calculating method with the lumbar spine is used in the thoracic QCT (shown in Fig. 1).

A significant association (0.85–0.99) between the thoracic and lumbar trabecular mineral density exists, which is confirmed by previous studies [21,33,34]. Based on this result, the thoracic BMD can translate to the lumbar equivalent values, and get the T score using the lumbar reference value. The formulas for translating the BMD value measured by thoracic QCT to the equivalent value with Lumbar QCT is: Lumbar BMD=0.8401×thoracic BMD+0.62 in female, and =0.8139×thoracic BMD+11.8 (mg/CM^3) in male, derived from the study data [21,23].

2.3. Phantomless assessment of the thoracic vertebral BMD using a routine heart scan

The clinical role of coronary calcium assessment by CT scan has undergone significant endorsement over the past 30 years [37]. The CT image from gated heart scans provide an opportunity to assess the CAC, and also thoracic BMD. As such, most of these studies were done without phantoms present. A phantomless thoracic BMD measurement would be a great advance in clinical practice. To date, three methods were used for the phantomless BMD measurement at spine: 1) Using an individual body tissue as a calibration reference, such as the paraspinal fat and psoas [38,39]; 2) Using a modified calibration factor (calibration curve) [40,41]; 3) Using the CTHU directly [42]. Although the standardization of CTHU was done by individual manufacturers, and the calibration procedure was performed before the row data reconstruction, a significant variation between scanners still exists [36,43]. The stabilization of CTHU can be influenced by numerous factors, including the scanner's model, scan algorithm parameters [44], patient's body size [35] and many other factors, which needs to be corrected before any quantitative assessment. Moreover, the attenuation

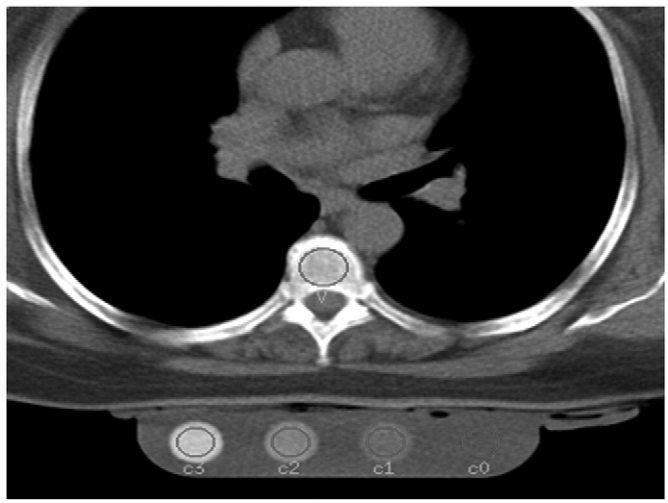

Fig. 1. The thoracic and lumbar BMD measurement by QCT. The bone mineral densities (mg/cm^3) in the three thoracic spines (from left main coronary artery level) were measured using the QCT technique. After selecting the spine slice, the cursor was located at the center of a spine or phantom rods automatically. The trabecular bone mineral densities (mg/cm^3) of 10 mm in thickness were displayed and recorded by computer. T scores were calculated using the reference values derived by the manufactory.

Please cite this article as: Mao SS, et al, Application of quantitative computed tomography for assessment of trabecular bone mineral density, microarchitecture and mechanica..., Clin Imaging (2015), http://dx.doi.org/10.1016/j.clinimag.2015.09.016

factor of patient's soft tissue (psoas and fat) is significantly different from bone, therefore, the accuracy may be affected by using the body anatomical markers. The calibration factor (ratio in true density phantom rod and CTHU, mg/cm^3/CTHU) may benefit BMD assessment, and the calibrating factors were established for most current scanners [36]. With this method, the CTHU was measured at three continuous thoracic spines described above. The center of sagittal or coronal spine image with a 6 to 10 mm in slice thickness is optimal to measure the CTHU using a CT workstation. The uniformed CTHU can be obtained from any CT workstation. The individual BMD can be obtained, CTHU×calibration factor (mg/cm^3) [36].

As the CAC scan protocol is standard for most medical centers, and the CTHU is relatively stable in a given scanner. By using the calibration factor to calculate BMD, the accuracy error has been decreased significantly. The variation of re-scan or re-measurement is <5%, <3% and <2% (CV) in phantom rods with a 50, 100 and 200 mg/cm^3 of CaHA respectively displayed by the prior study [36].

2.4. Thoracolumbar spine and hip BMD measurement from whole-body scan

2.4.1. Spine BMD measurement with QCT from a routine chest and abdomen CT images

Osteoporosis is a bone mineral metabolic disorder. Many diseases and conditions can influence the metabolic balance of the bone mineral materials (less absorption or faster turnover), such as renal disease [45,46], rheumatoid arthritis [47,48], heart failure and myocardial infarction [49–52], diabetes [53,54], chronic obstructive pulmonary disease [55–57], menopausal status [54,58], aging [59,60], nutrition disorder [61,62], and others [63,64]. The routine whole-body CT scan is an important medical imaging used for diagnosis and prognosis of these diseases and disorders. An analysis by the Organization for Economic and Cooperation and Development (OECD) found that there were about 80,000,000 CT examinations done in 2011, 60% of them underwent body CT scans in USA [65]. With those images one can obtain important information related diseases for diagnosis and prognosis, but typically ignores BMD and osteoporosis risk. Therefore, physicians can assess BMD and evaluate the fracture risk, as an additional evaluation for using these images with or without a calibration phantom using the QCT technique described above. The optimal results were obtained in most studies [33,34,36], including the chest [55,57,66], heart [21,23,36] and abdomen or pelvis CT scan [42,67,68]. A long calibration phantom (at least about 85 cm or longer, developed by Image Analysis, Columbia, KY, USA) is beneficial for the QCT BMD assessment with the whole-body scan [35].

2.4.2.1. Hip volumetric QCT with pelvis CT scan. In addition to the spine, the hip also is an important site of fracture, therefore, it is a major site for DXA BMD measurement [69,70]. The density of the femoral neck was used as an important parameter for the WHO FRAX 10-year fracture risk calculation [71]. Unlike thoracolumbar QCT, the hip volumetric QCT was rarely used to measure the bone density and calculate the T score. Comparing with the spine, the hip is more irregular in shape and smaller in size, which induces a problem to properly segment the trabecular bone. The hip QCT has been proposed and developed by using a CTHU threshold based-software to delineate the trabecular bone from the cortical bone [72,73]. The accuracy may be affected by the partial volume effect when using the threshold based-segmenting method. Manual segmentation and measurement of hip trabecular BMD was used at our center.

2.4.2.2. Hip area BMD measurement by CT two-dimensional projection images. The QCT X-Ray Absorptiometry (CTXA) analysis at the hip using pelvis CT images with a calibration phantom and software system was developed by Cann et al (Mindways Software, Inc, Austin, TX) [13,20]. This technique uses a two-dimensional projection (anterior-posterior) of CT three-dimensional formation with software to calculate the area bone density (mg/cm^2) in hip and femoral neck integral bone, just like the DXA method. When using the CTXA method, T scores should be calculated by conversion equations using the Hologic DXA-acquired NHANES III young normal data [20,74]. The hip CTXA are difficult to use routinely for the assessment of fracture risk due to it's high radiation dose and limitation of two-dimensional assessment. It can be used in cases with a restricted DXA availability or as an additional measure in cases already obtaining a pelvic CT study [13,20,75].

2.5. Extremity QCT measurement

The QCT technique has also been used for the peripheral BMD measurement using the spiral CT scan of upper [76,77] or lower extremity bone [8,76,78]. Whole-body spiral CT scan allow densitometric evaluations of the distal radius, tibia and other sites with good accuracy (R values 0.55-0.8 between QCT and DXA) [8,77,78]. A lower annual bone loss rate was found when compared to the central bone [76]. This method also provides a tool to further investigate cortical and trabecular bone microstructures. Nevertheless, it cannot become a routine screening method in QCT BMD assessment due to the high radiation and reduced accuracy for these applications [7]. It may be used as an additional investigation in patients requiring extremity CT scan for clinical purposes.

3. Analysis and results of QCT BMD assessment

3.1. Accuracy of the QCT

Compared to the cortical bone, trabecular bone density was significantly inhomogeneous within the individual or inter-spine locations. There was a stronger variation in CTHU within scanners, individuals and target objects, which results from the effect of beam hardening and partial volume artifacts [6,36]. With the calibration phantom technique, this effect can be partially reduced. A significant association ($R > 0.8$) between the true mass of the vertebral ash and the value measured by QCT was demonstrated [79,80]. However, the accurate determination of the trabecular mineral content is difficult with current QCT calibrating technique. Studies have shown a significant underestimation of QCT assessment (>20%) compared to the true values of vertebral ash [81]. The phantom rods consist of a solid resin matrix (water equivalent density, the attenuation is higher than the background of trabecular bone (red or yellow marrow), while a similar calcium material exists between the rod and spine. By using the higher reference values, measurements can be underestimated for the targets with the QCT. The accuracy may be improved with dual-energy CT scan [80]. We measured the CaHA concentration of phantom rods using the QCT technique. The biases from the true density of phantom rods and measured by the QCT were 4.0, 3.4 and 1.2% in the CaHA concentration in rods with CaCH of 50, 100 and 200 mg/cm^3 respectively, and no significant difference in accuracy within scanners made by various manufacturers in our recent study. Bligh's study showed a high accurate determination of torso phantom with a CV value range from 0.4% to 1.2% [82]. These results implied that the accuracy error may be less than 4% in most patients with QCT spine study, if we change the phantom material used to simulate the content of trabecular vertebrae (blood, yellow and red marrow and calcium).

3.2. Precision of the QCT in central, peripheral and CTDX assessment

The effective validation studies for the precision of QCT were completed within the scanners [81,82], calibration phantoms [16,82], studies [21,36], inter- or intro-readers [21,36], in short- or long-term [78,82,83] and scan parameters [82]. Overall, high-precision results were found in most studies. The average coefficient variation of a precision error (CV% by RMS or SD/mean methods) was <3% from 1.8 to 4.0% in most studies [8,21,38,77,78,82,83]. The precision error among scan parameters can be limited to 2% of CV. These parameters include the scan voltage, tube

Please cite this article as: Mao SS, et al, Application of quantitative computed tomography for assessment of trabecular bone mineral density, microarchitecture and mechanica..., Clin Imaging (2015), http://dx.doi.org/10.1016/j.clinimag.2015.09.016

temperature during imaging, scan table height, pitch (table increment speed), and reconstruction algorithms [82]. In the study cohort with a low BMD, the precision error is higher than the patients with a higher density. The peripheral sites (radius, tibia or other sites) have a higher precision error (2–5% of CV) when comparing with the central structures [8,77,78]. In general, with the calibration phantom employment, the precision error of QCT can be limited effectively. The QCT volumetric density assessment in the hip has also shown a very low (<2%) precision error [84,85]. All studies indicated that there was a significant association between the hip CTXA and DXA (r>0.95) with a high precision (CV <2%) [13,20].

The long term precision error of the CaHA content in phantom rod was studied at our laboratory by using 62 re-scan patients in a three- and half year follow up interval. The precision error was 2.04% (95% CI:1.49 to 4.15%, RMS) in rods with 100 and 200 mg/cm^3 of CaHA.

We conclude that the QCT technique has a high precision in central or peripheral bone density assessment.

3.3. Agreement between the QCT and DXA in diagnosing osteoporosis

The association and agreement between the QCT lumbar and the DXA lumbar or hip assessment had been reported previously [22,86–88]. Most studies demonstrated a moderate or good association (r<0.75) and a fair to moderate agreement (Kappa value <0.6) in detecting bone status between the hip or lumbar DXA and lumbar QCT [22,86,87]. Studies indicated that the QCT had a higher ability to detect osteoporosis than DXA [22,86,87]. These comparison results imply that both the QCT and DXA cannot be interchangeably used. The reference values of DXA and QCT never were normalized sufficiently.

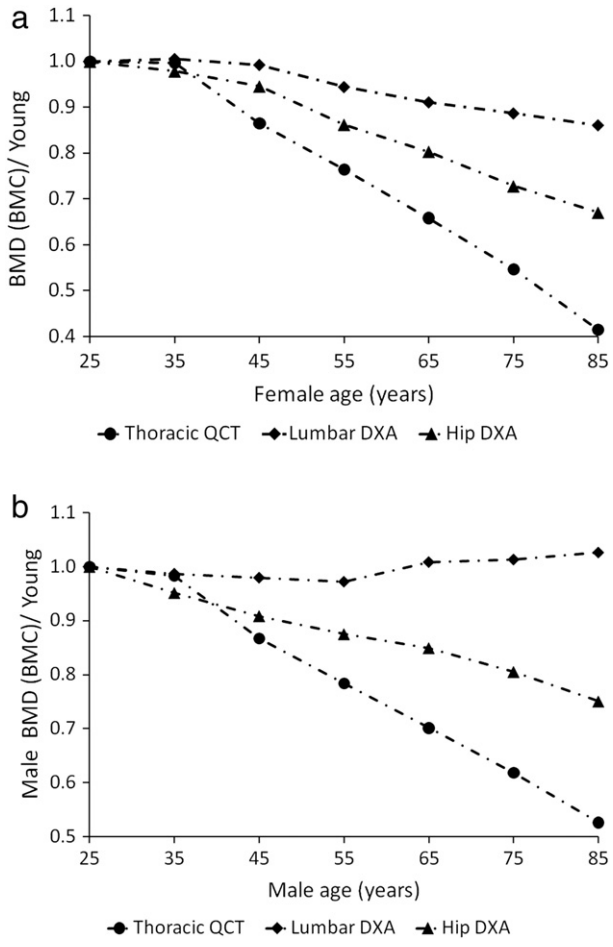

Fig. 2. A and B. Comparison of the BMD change with aging within thoracic QCT, lumbar DXA and neck of hip DXA. From Budoff [21] and Looker [74,92].

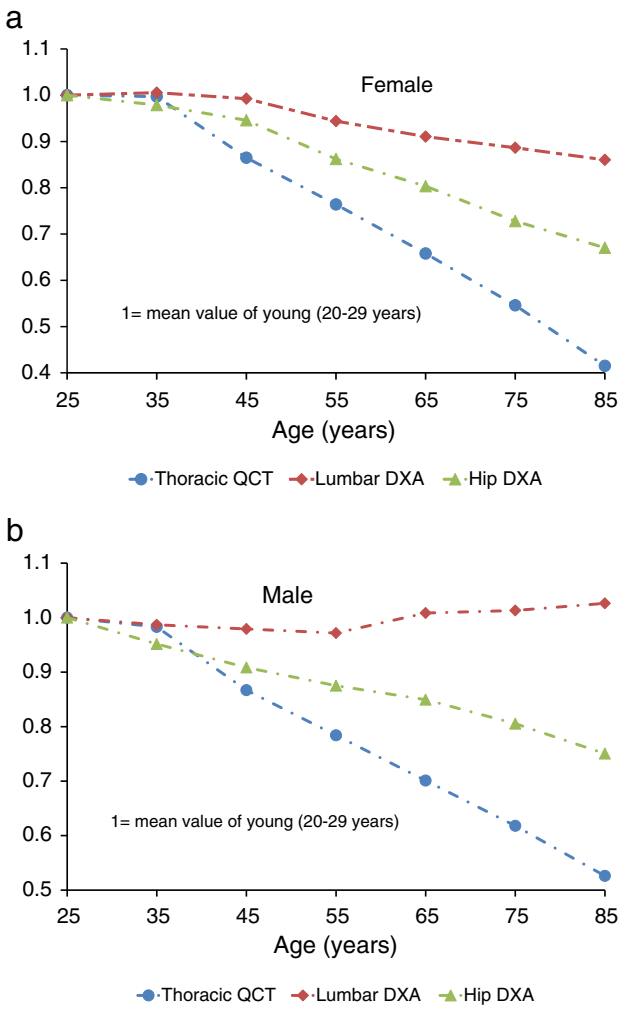

Fig. 3. The curve of bone density of the first thoracic to the fifth lumbar spine [35].

3.4. Detecting the annual decrease rate between QCT and DXA

Sensitive detection of the bone loss is very important to monitor the bone density change. The central region (vertebrae and femur) is the optimal location to monitor the BMD changes, and also is the area more frequently involved in the fracture [89,90]. The bone annual loss rate is variable with the study populations and methods used. A large number of the comparison studies were completed between the DXA and QCT in the annual change rate of bone density [22,87,88,91]. Those rates can be assessed by using longitudinal or cross sectional studies. Review of the reference data base by Budoff et all [21] and NHANES III [74,92] showed the bone density change from 30 to >80 years were -59%, -14% and -33% in women, -48%, +4% and -25% in men in the QCT thoracic, DXA lumbar and femoral neck measurement respectively (shown on Fig. 2). A faster decline in BMD with aging was found in the QCT thoracic than the DXA lumbar and femoral neck measurement. The conclusion is clear that the QCT is a more sensitive method for detecting the bone density change in comparing with the DXA [22,88,91,93,94].

3.5. Associations within lumbar, thoracic and other sites's QCT in BMD measurement and agreement in diagnosis of osteoporosis by the T score

The central skeleton, such as spine and proximal femur, was commonly used to assess the BMD by DXA. However, only the lumbar QCT was commonly used in clinical practice. The associations between the lumbar

Table 1
Association (T scores) within thoracic, lumbar, ilium and femur QCT BMD measurement

Kappa Value	L1-3		LR Ilium		LR Hip	
T<2.5	R	kappa	R	kappa	R	kappa
3 T	0.78	0.77	0.74	0.73	0.56	0.48
L1-3			0.64	0.63	0.44	0.40
Ilium					0.52	0.46

and thoracic spine, as well as hip and/or peripheral bones were studied previously [23,35]. There were a significant associations between L1-3 (lumbar spine 1-3) and any individual vertebrae from the first thoracic to the fifth lumbar spine (R value, from 0.62 to 0.98, $P<.001$). Significant differences exist within most adjacent vertebrae ($P<.05$). The T1 has the largest, and L3 has the smallest BMD value ($P<.05$) when comparing with 17 thoracic and lumbar spines. From the T1 to L3, the BMD progressively decreased (shown on Fig. 3) and increased from L4 and L5. A significant association between the mean value of 3 T (three continuous thoracic spines from the slice level in containing left main coronary artery) and L1-3 with a 0.89 of R values was found in both genders. Both 3 T and L1-3 were used in the QCT assessment with a routine heart or lumbar scan [35].

In our knowledge, no association in the BMD value or agreement in the T score between the lumbar and hip or peripheral measurement using QCT was documented to date. We analyzed the trabecular BMD in 62 cases with the thoracic, lumbar, ilium and hip in patients with a chest, abdomen and pelvis CT scan. The trabecular BMD in 3 T and L1-3 was measured with QCT technique. The phantom rods and trabeculae of the ilium and the hip were segmented manually, and the BMD was calculated by using a calibrating factor derived from the phantom rods. All BMD of the 3 T, iliums and hips were translated to the lumbar- equivalent value, then the T scores were derived using the lumbar reference by the Image analysis (Columbia, KY, USA). The results were listed in the Table 1.

The result indicates that the substantial association and agreement exist within thoracic, lumbar and ilium bone, but only a moderate association and agreement exist between the hip with spine and ilium.

From above results, we conclude that a significant association, but difference exists between the lumbar and thoracic spines. A similar result (T score) can be obtained with the ilium, thoracic and lumbar spine in predicting osteoporosis, when using the same standard reference (translating the thoracic to the lumbar or reverse). The lumbar (or thoracic) and hip QCT cannot be interchangeably even using the lumbar-equivalent BMD values.

3.6. Comparison of annual change rate of bone density between the QCT lumbar and thoracic or peripheral measurements

In a QCT study by Li et al [23], the annual loss rate is 1.0% and 1.1%/year ($P=.16$) in male, 1.4 and 1.5%/year ($P<.001$) in female for thoracic and lumbar trabeculae respectively with good association ($r=0.87$, $P<.001$). The result implies a similar bone change rate in both thoracic and lumbar spines.

The agreement (increase or decrease) between the thoracic and lumbar spine on the BMD change in a three-year follow-up period in 500 cases (female 238) with both thoracic and lumbar re-scan was reported. The result indicated that there was a moderate (kappa value of 0.59) and a substantial (0.69) agreement of BMD change between the thoracic and lumbar spine in women and men respectively. The combination of both thoracic and lumbar QCT may improve the accuracy in detecting the BMD change, which needs to be validated by a continuous study.

Riggs et al investigated the annual loss rate of bone density in a large population sample. The result indicated that the annual loss rate of the lumbar spine is 2–6 folds to that of the peripheral sites at distal radius and tibia with a trabecular QCT measurement [76]. Studies indicated that the trabecular QCT of spinal bone displayed a strong capability for assessment of the bone loss rate and for discrimination of osteoporotic vertebral fractures. In comparison to the central bone, the peripheral bone had the weakest capability for these applications [7,76,95].

In summation, a significant variation in the loss rate of bone mineral density exists within the different sites of skeletons. The lumbar spine is a more sensitive structure to monitor the BMD change.

3.7. Comparing the bone loss rate between the trabecular and cortical bone

In the central sites (spine and hip), the trabecular bone consists of a major part (>70% in vertebrae) [95,96], and is a fast metabolic component [97]. There was a strong variation in the bone annual loss rate in the study cohort with different age and clinical implications. Overall, the trabecular bone has a 3–10 fold bone loss rate compared to the cortical bone [76,95,97–99].

3.8. The feasibility in predicting osteoporosis fracture using the QCT

The main aim of QCT study is to predict the fracture risk in patients with osteoporosis, and monitor the BMD and structure changes related to aging, disease and medication. Studies for predicting fracture were reported [77,94,100,101]. The FRAX 10-year fracture risk calculation tool was established by Kanis et al. using the hip DXA [71]. This model provided a possibility in the assessment of fracture risk for both men and women by the integration of clinical risk factors alone and/or in combination with BMD measured by DXA. The comparative study of QCT and DXA was also completed. The results indicated that the QCT is a more sensitive method to predict the fracture risk [77,94,100,101]. An advanced investigation, just like DXA, was necessary to develop a model for assessing the fracture possibility in the spine or hip by using relative factors, which include the BMD, microarchitectural and mechanical data from QCT assessment, and important clinical applications.

3.9. Follow-up time using the QCT

Monitoring osteoporosis and atherosclerosis is very important to prevent bone fracture and coronary artery disease. Currently, coronary calcium scan as well as coronary angiography scan has become an important methodology for screening or monitoring patients with suspected CAD or coronary revascularization [37]. The optimal follow-up interval using CAC scan, QCT and DXA for patients with osteoporosis and atherosclerosis has been still ambiguous [102,103]. A study by Lenora et al. [104] displayed the follow-up intervals (least significant change/median rate of a BMD change) in both women and men as 8 years and 13 years, respectively, by using a DXA scanner, 3 and 32 years by using a lunar Prodigy scanner for total hip and lumbar spine respectively. A Quantitative ultrasonography study indicated that no significant difference of BMD was found in an eight-year interval in a cohort consisting of healthy, older, postmenopausal women [105]. The revised and expanded recommendations in 2010 by the U.S. Preventive Services Task Force (USPSTF) underscore the need for more screening of the bone density [106]. The time interval of monitoring bone mineral density relies on both the precision error of the method used and the rate of bone loss for the population studied. To address this key issue, it is important to keep in mind that the bone density and the rate of bone loss are varied according to age of population, gender, diseases, medication and test sites. Of note, the spine trabecular bone is a more sensitive site compared to the peripheral and cortical bone [7,107]. In the general population, the loss rate of a spine trabecular bone is approximately 1% per year in young or mid aging persons, 2% in elderly, and rapid in early menopausal women or patients with an abnormal mineral metabolism [23,35,76,108].

Based on Gluerr et al the "monitoring time interval" (MTI) formula was considered as [109]: The follow-up time needed to exceed the least significant change (LSC=2.77×maximal CT long-term precision error, in 95% CI) I.E., LSC÷median change per annum [109]. As a result, the LSC is 11.3 [2.77× 4.09 (in maximal CT long-term precision error, in 95% CI, described above)] by using the formula. According to two study data [21,23], the

Table 2
Comparison of clinical application, spatial resolution and radiation dose within pQCT, μCT and MDCT

Scanner	Skeletal Sites	Spatial Resolution (μm)	Effective Dose (mSv)	Reference
μCT	Specimens ex vivo	0.3–100 Isotropic	17–112 or more	[136,137,141]
pQCT	Extremities specimens	41–123 Isotropic	<0.01	[10,21,120]
MDCT	All sites of body specimens	195 in plane 500–700 through plane	1–4 for lumbar SCAN	[8,9,142]

aging annual change rate of a thoracic or lumbar spine is about 1–2% in average, and the monitoring time interval is about 6–12 years by using a spine QCT. We tested the MTI formula using a total of 500 subjects (mean age 65 years, 238 women) with a re-scan interval of 3 years. The rate of BMD change is larger than 11.3% in 18% and 8.8%, and larger than 4.09% in 63% and 62% in women and men respectively. This result means LSE of 11.3% may be too long due to the large value of precision errors in the QCT study. If using the 4.09% as borderline of significant change in the rate, the time of follow up can be shortened to 3 years in this study cohort.

The guidelines of CAC scan recommended five-year interval of reassessment for those with a positive test result of atherosclerosis, and every 5–10 years for those with a negative test result [110]. Based on the result deduced from this study, it may be reasonable to suggest using the same time interval, and the same CACs image to monitor both osteoporosis and atherosclerosis in the general population.

4. Assessment of the trabecular microarchitecture

4.1. Assessment of the bone trabecular microarchitecture with peripheral QCT (pQCT)

The high resolution pQCT (HR-pQCT) is primarily installed at major research centers and clinical radiology departments [111–114]. Using the high spatial resolution image (100 μm or less in pixel size), the resolution obtained is close to or smaller than the average trabecular thickness (100–150 μm) [12]. It can separate the periosteal boundary and segment the cortical and trabecular compartments. The ratio of mineralized bone volume to total volume [BV/TV]), trabecular thickness (Tb.Th), trabecular separation (Tb.Sp), trabecular number (Tb.N), connectivity and structure model index (SMI) and the volumetric BMD can be evaluated accurately at the extremities [115].

Studies indicated a high agreement between μQCT (microCT) and pQCT in the volumetric BMD (<1% in CV, and $r^2 = 0.8$), and the microarchitecture measures (coefficient of variation in 4% to 5%) [111,112,116–119].

4.2. Assessment of the BMD, trabecular microarchitecture with μQCT

The μQCT is also an X-ray based image. Just like the QCT, various calibration phantoms or theoretical calculations were established to derive BMD from CT attenuation value [120,121].

This scanner uses polychromatic X-ray source, which produces highest spatial resolution images of less 10 μm [12,122]. μQCT can effectively quantify the volumetric BMD and the microarchitecture of cortical and trabecular bone. The utility of the μQCT is similar to the pQCT and it is more sensitive to display the detail of microarchitecture with a high accuracy and precision [123–126].

In comparing the pQCT and MDCT, μQCT is used only for bone specimens and small animal model's imaging for evaluating bone microarchitecture in the laboratory [127,128] due to it's high radiation dose [129,130].

4.3. Assessment of the trabecular microarchitecture with MDCT

In current, the rotation speed of MDCT of the X-ray tube is less than 300 milliseconds with less than a millimeter in spatial resolution. With a small field of view of 10 centimeters, the in plane and through plane spatial resolution can close to 200–500 um, is larger, but close to the trabecular size (100–150 μm) [12].

The BV/TV, Tb.N, Tb.Th, and Tb.Sp, connectivity and structure model index (SMI) are calculated two-dimensionally using plate model assumptions [131,132] or direct three-dimensional measures [133]. Due to the lower spatial resolution comparing with the pQCT or μQCT, the partial volume effect is relatively large. Studies have shown a moderate correlation between the MDCT and μQCT in trabecular microstructure assessment (r=.44–0.99) [132,134]. The advantage of the MDCT technique is that both the central or peripheral regions of the skeleton can be assessed, such as the spine, proximal femur and extremity [132,133,135]. Studies indicated that the BV/TV and SMI measured from lumbar spine by MDCT provided a superior result in predicting fracture risk and therapeutic evaluation than BMD measurement with DXA or QCT [133,136]. Currently, the bone microarchitecture assessment of the lumbar spine by using MDCT is still limited due to radiation dose concern. The common utilities, spatial resolution and radiation dose of pQCT, μQCT and MDCT are listed in the Table 2.

5. Assessment of bone mechanical property

The assessment of trabecular BMD and microarchitecture directly reflects the important pathological changes in of osteoporosis, low bone mass and microarchitecture deterioration. Both of them are generally related to material property and structure characteristic, and only partly to the mechanical behavior. Hence, the BMD and microarchitecture based mechanical assessment (finite-element analysis, FEA) can estimate the bone strength or stiffness effectively, that related the skeleton fragility fracture directly.

FEA is a well-established method as a computational tool for estimating the complex engineering problems, and has also been a valuable tool for investigating biological problems, such as for bone mechanical test. It includes the use of mesh generation techniques that can divide a *complex problem* into finite elements. Application of image based on FEA initiated was first utilized in the field of orthopedic biomechanics [137,138] in the 1970s. During the past two decades, the usage has been growing rapidly following the revolution of MDCT technique and increased awareness of osteoporosis universally [138,139].

The strategy of image-based FEA is integrating the data of material (BMD) or microarchitecture behavior (bone volume fraction-BV/TV, plate-like or rod-like trabecula) [121,138–141] and the geometric distribution of both through simulated experimental models. Those simulated strength models based on CT or MRI images included various bones (spine, hip, radius and tibia) validated by vitro studies [84,142–144]. The two- or three-dimensional model map of finite element contained the pixel or voxel data of BMD or microarchitecture, and combined geometric behaviors that related to the orientation of loading force. Therefore, the FEA provides a comprehensive assessment of bone strength or stiffness.

Studies indicated that the MDCT is of potential ability to be used for the FEA in the vitro and vivo tests [139,145]. MDCT based FEA provides the most reliable role tool to predict the bone strength [138,140,146], risk of fracture [139,147,148] and it's also more sensitive to monitor anti-osteoporosis [142,149] when compared to any of the conventionally used densitometric and microstructure standards. FEA methodology using the MDCT exhibited high reproducibility with a low precision error of 1.51% in assessing the femoral bone assessment [141]. Finite-element methods are becoming increasingly popular for quantifying

Please cite this article as: Mao SS, et al, Application of quantitative computed tomography for assessment of trabecular bone mineral density, microarchitecture and mechanica..., Clin Imaging (2015), http://dx.doi.org/10.1016/j.clinimag.2015.09.016

the mechanical properties. Currently, MDCT scans are routinely employed for a wide range of diagnostic indications. The authors believe that the MDCT based density, structure and strength assessment will playing an important role of in the bone health management in future.

6. Summary

QCT is an optimal method of measuring bone mineral density for detecting osteoporosis and monitoring the age-, disease-and medicine-related BMD change accurately. The trabecular bone mineral density, microarchitectural and mechanical assessment can be obtained simultaneously with the current routine MDCT image. Combinations of all information from the bone density measurement, microarchitectural and mechanical assessment may improve the result in estimating the bone strength, predicting risk of fragility fracture and management of bone health. The vertebral trabeculae is an optimal structure for the BMD measurement. With MDCT body routine scan images, such as heart, chest, abdomen, pelvis and peripheral sites, the BMD can be assessed accurately as additional clinical information using the QCT. Using the QCT calibration technique, the variation within the scanners, patients, and anatomical structures can be limited, and the results become interchangeable between scanners [36]. Furthermore, the modified QCT methodology (phantomless) also is acceptable to assess BMD, but the calibration factors need to be calculated for a given scanner before or after the studies [36,40,41]. The psoas or fat tissue of paravertibrae can be used as a calibration mark [38,39]. Further studies well be needed to demonstrate the role of QCT in predicting fracture risk and monitoring anti-osteoporosis by using BMD, micro-architectural and mechanical assessments. Combining the three methods and both structure (cortical and trabecular bone) evaluations with MDCT may need for increased utilization in this context.

References

[1] Ammann P, Rizzoli R. Bone strength and its determinants. Osteoporos Int 2003; 14(Suppl. 3):S13–8.
[2] Lang TF. Summary of research issues in imaging and noninvasive bone measurement. Bone 1998;22:159S–61S.
[3] World health organization. Assessment of the fracture risk and its application to screening for postmeneopausal osteoporosis. Report no WHO technical report series 843 GW; 1994. p. 1–129.
[4] Kanis JA, Gluer CC. An update on the diagnosis and assessment of osteoporosis with densitometry. Committee of Scientific Advisors, International Osteoporosis Foundation. Osteoporos Int 2000;11:192–202.
[5] Yu EW, Bouxsein ML, Roy AE, Baldwin C, Cange A, Neer RM, et al. Bone loss after bariatric surgery: discordant results between DXA and QCT bone density. J Bone Miner Res 2014;29:542–50.
[6] Cann CE, Genant HK. Precise measurement of vertebral mineral content using computed tomography. J Comput Assist Tomogr 1980;4:493–500.
[7] Grampp S, Jergas M, Lang P, Steiner E, Fuerst T, Gluer CC, et al. Quantitative CT assessment of the lumbar spine and radius in patients with osteoporosis. AJR Am J Roentgenol 1996;167:133–40.
[8] Johnston JD, McLennan CE, Hunter DJ, Wilson DR. In vivo precision of a depth-specific topographic mapping technique in the CT analysis of osteoarthritic and normal proximal tibial subchondral bone density. Skelet Radiol 2011;40:1057–64.
[9] Majumdar S, Newitt D, Jergas M, Gies A, Chiu E, Osman D, et al. Evaluation of technical factors affecting the quantification of trabecular bone structure using magnetic resonance imaging. Bone 1995;17:417–30.
[10] Mueller D, Link TM, Monetti R, Bauer J, Boehm H, Seifert-Klauss V, et al. The 3D-based scaling index algorithm: a new structure measure to analyze trabecular bone architecture in high-resolution MR images in vivo. Osteoporos Int 2006;17:1483–93.
[11] Huopio J, Kroger H, Honkanen R, Jurvelin J, Saarikoski S, Alhava E. Calcaneal ultrasound predicts early postmenopausal fractures as well as axial BMD. A prospective study of 422 women. Osteoporos Int 2004;15:190–5.
[12] Burghardt AJ, Link TM, Majumdar S. High-resolution computed tomography for clinical imaging of bone microarchitecture. Clin Orthop Relat Res 2011;469: 2179–93.
[13] Cann CE, Adams JE, Brown JK, Brett AD. CTXA hip—an extension of classical DXA measurements using quantitative CT. PLoS One 2014;9:e91904.
[14] OECD. Organisation for economic Co-operation and development health statistics; 2014.
[15] Engelke K, Grampp S, Gluer CC, Jergas M, Yang SO, Genant HK. Significance of QCT bone mineral density and its standard deviation as parameters to evaluate osteoporosis. J Comput Assist Tomogr 1995;19:111–6.
[16] Faulkner KG, Gluer CC, Grampp S, Genant HK. Cross-calibration of liquid and solid QCT calibration standards: corrections to the UCSF normative data. Osteoporos Int 1993;3:36–42.
[17] Kalender WA. A phantom for standardization and quality control in spinal bone mineral measurements by QCT and DXA: design considerations and specifications. Med Phys 1992;19:583–6.
[18] ACR. American College Of Radiology practice guideline for the performance of quantitative computed tomography; 2008.
[19] Yoshihashi AK, Drake AJ, Shakir KM. Ward's triangle bone mineral density determined by dual-energy x-ray absorptiometry is a sensitive indicator of osteoporosis. Endocr Pract 1998;4:69–72.
[20] Khoo BC, Brown K, Cann C, Zhu K, Henzell S, Low V, et al. Comparison of QCT-derived and DXA-derived areal bone mineral density and T scores. Osteoporos Int 2009;20:1539–45.
[21] Budoff MJ, Hamirani YS, Gao YL, Ismaeel H, Flores FR, Child J, et al. Measurement of thoracic bone mineral density with quantitative CT. Radiology 2010;257:434–40.
[22] Grampp S, Genant HK, Mathur A, Lang P, Jergas M, Takada M, et al. Comparisons of noninvasive bone mineral measurements in assessing age-related loss, fracture discrimination, and diagnostic classification. J Bone Miner Res 1997;12:697–711.
[23] Li D, Mao SS, Khazai B, Hyder JA, Allison M, McClelland R, et al. Noncontrast cardiac computed tomography image-based vertebral bone mineral density: the Multi-Ethnic Study of Atherosclerosis (MESA). Acad Radiol 2013;20:621–7.
[24] Kado DM, Browner WS, Blackwell T, Gore R, Cummings SR. Rate of bone loss is associated with mortality in older women: a prospective study. J Bone Miner Res 2000;15:1974–80.
[25] Chow JT, Khosla S, Melton LJ, Atkinson EJ, Camp JJ, Kearns AE. Abdominal aortic calcification, BMD, and bone microstructure: a population-based study. J Bone Miner Res 2008;23:1601–12.
[26] Sambrook P, Cooper C. Osteoporosis. Lancet 2006;367:2010–8.
[27] Bild DE, Detrano R, Peterson D, Guerci A, Liu K, Shahar E, et al. Ethnic differences in coronary calcification: the Multi-Ethnic Study of Atherosclerosis (MESA). Circulation 2005;111:1313–20.
[28] ACR-SSR. Practice guideline for the performance of dual energy x-ray absorptiometry (DXA); 2008[Accessed October 20, 2014].
[29] Leib ES, Lewiecki EM, Binkley N, Hamdy RC, International Society for Clinical D. Official positions of the International Society for Clinical Densitometry. South Med J 2004;97:107–10.
[30] Lim LS, Hoeksema LJ, Sherin K. Screening for osteoporosis in the adult U.S. population: ACPM position statement on preventive practice. Am J Prev Med 2009;36:366–75.
[31] Richards PJ, George J, Metelko M, Brown M. Spine computed tomography doses and cancer induction. Spine 2010;35:430–3.
[32] Hospers IC, van der Laan JG, Zeebregts CJ, Nieboer P, Wolffenbuttel BH, Dierckx RA, et al. Vertebral fracture assessment in supine position: comparison by using conventional semiquantitative radiography and visual radiography. Radiology 2009; 251:822–8.
[33] Lenchik L, Shi R, Register TC, Beck SR, Langefeld CD, Carr JJ. Measurement of trabecular bone mineral density in the thoracic spine using cardiac gated quantitative computed tomography. J Comput Assist Tomogr 2004;28:134–9.
[34] Wong M, Papa A, Lang T, Hodis HN, Labree L, Detrano R. Validation of thoracic quantitative computed tomography as a method to measure bone mineral density. Calcif Tissue Int 2005;76:7–10.
[35] Budoff MJ, Khairallah W, Li D, Gao YL, Ismaeel H, Flores F, et al. Trabecular bone mineral density measurement using thoracic and lumbar quantitative computed tomography. Acad Radiol 2012;19:179–83.
[36] Budoff MJ, Malpeso JM, Zeb I, Gao YL, Li D, Choi TY, et al. Measurement of phantomless thoracic bone mineral density on coronary artery calcium CT scans acquired with various CT scanner models. Radiology 2013;267:830–6.
[37] Budoff MJ, Cohen MC, Garcia MJ, Hodgson JM, Hundley WG, Lima JA, et al. ACCF/AHA clinical competence statement on cardiac imaging with computed tomography and magnetic resonance. Circulation 2005;112:598–617.
[38] Mueller DK, Kutscherenko A, Bartel H, Vlassenbroek A, Ourednicek P, Erckenbrecht J. Phantom-less QCT BMD system as screening tool for osteoporosis without additional radiation. Eur J Radiol 2011;79:375–81.
[39] Gudmundsdottir H, Jonsdottir B, Kristinsson S, Johannesson A, Goodenough D, Sigurdsson G. Vertebral bone density in Icelandic women using quantitative computed tomography without an external reference phantom. Osteoporos Int 1993;3:84–9.
[40] Habashy AH, Yan X, Brown JK, Xiong X, Kaste SC. Estimation of bone mineral density in children from diagnostic CT images: a comparison of methods with and without an internal calibration standard. Bone 2011;48:1087–94.
[41] Summers RM, Baecher N, Yao J, Liu J, Pickhardt PJ, Choi JR, et al. Feasibility of simultaneous computed tomographic colonography and fully automated bone mineral densitometry in a single examination. J Comput Assist Tomogr 2011;35:212–6.
[42] Pickhardt PJ, Lee LJ, del Rio AM, Lauder T, Bruce RJ, Summers RM, et al. Simultaneous screening for osteoporosis at CT colonography: bone mineral density assessment using MDCT attenuation techniques compared with the DXA reference standard. J Bone Miner Res 2011;26:2194–203.
[43] Levi C, Gray JE, McCullough EC, Hattery RR. The unreliability of CT numbers as absolute values. AJR Am J Roentgenol 1982;139:443–7.
[44] McCollough CH, Ulzheimer S, Halliburton SS, Shanneik K, White RD, Kalender WA. Coronary artery calcium: a multi-institutional, multimanufacturer international standard for quantification at cardiac CT. Radiology 2007;243:527–38.
[45] Molnar MZ, Naser MS, Rhee CM, Kalantar-Zadeh K, Bunnapradist S. Bone and mineral disorders after kidney transplantation: therapeutic strategies. Transplant Rev 2014;28:56–62.

Please cite this article as: Mao SS, et al, Application of quantitative computed tomography for assessment of trabecular bone mineral density, microarchitecture and mechanica..., Clin Imaging (2015), http://dx.doi.org/10.1016/j.clinimag.2015.09.016

[46] Kaji H, Yamauchi M, Yamaguchi T, Shigematsu T, Sugimoto T. Mild renal dysfunction is a risk factor for a decrease in bone mineral density and vertebral fractures in Japanese postmenopausal women. J Clin Endocrinol Metab 2010;95:4635–42.
[47] Lodder MC, de Jong Z, Kostense PJ, Molenaar ET, Staal K, Voskuyl AE, et al. Bone mineral density in patients with rheumatoid arthritis: relation between disease severity and low bone mineral density. Ann Rheum Dis 2004;63:1576–80.
[48] Lee JY, Harvey WF, Price LL, Paulus JK, Dawson-Hughes B, McAlindon TE. Relationship of bone mineral density to progression of knee osteoarthritis. Arthritis Rheum 2013;65:1541–6.
[49] Majumdar SR, Ezekowitz JA, Lix LM, Leslie WD. Heart failure is a clinically and densitometrically independent risk factor for osteoporotic fractures: population-based cohort study of 45,509 subjects. J Clin Endocrinol Metab 2012;97:1179–86.
[50] Terrovitis J, Zotos P, Kaldara E, Diakos N, Tseliou E, Vakrou S, et al. Bone mass loss in chronic heart failure is associated with secondary hyperparathyroidism and has prognostic significance. Eur J Heart Fail 2012;14:326–32.
[51] Wiklund P, Nordstrom A, Jansson JH, Weinehall L, Nordstrom P. Low bone mineral density is associated with increased risk for myocardial infarction in men and women. Osteoporos Int 2012;23:963–70.
[52] Pfister R, Michels G, Sharp SJ, Luben R, Wareham NJ, Khaw KT. Low bone mineral density predicts incident heart failure in men and women: the EPIC (European Prospective Investigation into Cancer and Nutrition)-Norfolk prospective study. JACC Heart Fail 2014;2:380–9.
[53] Shu A, Yin MT, Stein E, Cremers S, Dworakowski E, Ives R, et al. Bone structure and turnover in type 2 diabetes mellitus. Osteoporos Int 2012;23:635–41.
[54] Bilezikian JP, Josse RG, Eastell R, Lewiecki EM, Miller CG, Wooddell M, et al. Rosiglitazone decreases bone mineral density and increases bone turnover in postmenopausal women with type 2 diabetes mellitus. J Clin Endocrinol Metab 2013;98:1519–28.
[55] Kiyokawa H, Muro S, Oguma T, Sato S, Tanabe N, Takahashi T, et al. Impact of COPD exacerbations on osteoporosis assessed by chest CT scan. COPD 2012;9:235–42.
[56] Wang TY, Lo YL, Chou PC, Chung FT, Lin SM, Lin TY, et al. Associated bone mineral density and obstructive sleep apnea in chronic obstructive pulmonary disease. Int J Chron Obstruct Pulmon Dis 2015;10:231–7.
[57] Looker AC. Relationship between femur neck bone mineral density and prevalent chronic obstructive pulmonary disease (COPD) or COPD mortality in older non-Hispanic white adults from NHANES III. Osteoporos Int 2014;25:1043–52.
[58] Montalcini T, Gallotti P, Coppola A, Zambianchi V, Fodaro M, Galliera E, et al. Association between low C-peptide and low lumbar bone mineral density in postmenopausal women without diabetes. Osteoporos Int 2015;26:1639–46.
[59] Sheu Y, Bunker CH, Jonnalagadda P, Cvejkus RK, Patrick AL, Wheeler VW, et al. Rates of and risk factors for trabecular and cortical BMD loss in middle-aged and elderly African-ancestry men. J Bone Miner Res 2015;30:464–74.
[60] Giusti A, Bianchi G. Treatment of primary osteoporosis in men. Clin Interv Aging 2015;10:105–15.
[61] Niimi R, Kono T, Nishihara A, Hasegawa M, Matsumine A, Kono T, et al. Analysis of daily teriparatide treatment for osteoporosis in men. Osteoporos Int 2015;26:1303–9.
[62] Joo NS, Dawson-Hughes B, Kim YS, Oh K, Yeum KJ. Impact of calcium and vitamin D insufficiencies on serum parathyroid hormone and bone mineral density: analysis of the fourth and fifth Korea National Health and Nutrition Examination Survey (KNHANES IV-3, 2009 and KNHANES V-1, 2010). J Bone Miner Res 2013;28:764–70.
[63] Bellasi A, Zona S, Orlando G, Carli F, Ligabue G, Rochira V, et al. Inverse correlation between vascular calcification and bone mineral density in human immunodeficiency virus-infected patients. Calcif Tissue Int 2013;93:413–8.
[64] Canepa M, Ameri P, AlGhatrif M, Pestelli G, Milaneschi Y, Strait JB, et al. Role of bone mineral density in the inverse relationship between body size and aortic calcification: results from the Baltimore Longitudinal Study of Aging. Atherosclerosis 2014;235:169–75.
[65] OECD, Health at a Glance,. OECD indicators. OECD Publishing; 2011[http://dx.doi.org/10.1787/health_glance-2011-en].
[66] Romme EA, Murchison JT, Phang KF, Jansen FH, Rutten EP, Wouters EF, et al. Bone attenuation on routine chest CT correlates with bone mineral density on DXA in patients with COPD. J Bone Miner Res 2012;27:2338–43.
[67] Papadakis AE, Karantanas AH, Papadokostakis G, Petinellis E, Damilakis J. Can abdominal multi-detector CT diagnose spinal osteoporosis? Eur Radiol 2009;19:172–6.
[68] Bauer JS, Henning TD, Mueller D, Lu Y, Majumdar S, Link TM. Volumetric quantitative CT of the spine and hip derived from contrast-enhanced MDCT: conversion factors. AJR Am J Roentgenol 2007;188:1294–301.
[69] Kanis JA, McCloskey EV, Johansson H, Oden A, Melton LJ, Khaltaev N. A reference standard for the description of osteoporosis. Bone 2008;42:467–75.
[70] Nordstrom P, Gustafson Y, Michaelsson K, Nordstrom A. Length of hospital stay after hip fracture and short term risk of death after discharge: a total cohort study in Sweden. BMJ 2015;350:h696.
[71] Kanis JA, Johnell O, Oden A, Johansson H, McCloskey E. FRAX and the assessment of fracture probability in men and women from the UK. Osteoporos Int 2008;19:385–97.
[72] Genant HK, Engelke K, Prevrhal S. Advanced CT bone imaging in osteoporosis. Rheumatology 2008;47(Suppl. 4):iv9–iv16.
[73] Amstrup AK, Jakobsen NF, Lomholt S, Sikjaer T, Mosekilde L, Rejnmark L. Inverse correlation at the Hip between areal bone mineral density measured by dual-energy X-ray absorptiometry and cortical volumetric bone mineral density measured by quantitative computed tomography. J Clin Densitom 2015 [in press].
[74] Looker AC, Borrud LG, Hughes JP, Fan B, Shepherd JA, Sherman M. Total body bone area, bone mineral content, and bone mineral density for individuals aged 8 years and over: United States, 1999–2006. National Center for Health Statistics. Vital Health Stat 11 2013(253):1–77.
[75] Keyak JH, Sigurdsson S, Karlsdottir G, Oskarsdottir D, Sigmarsdottir A, Zhao S, et al. Male-female differences in the association between incident hip fracture and proximal femoral strength: a finite element analysis study. Bone 2011;48:1239–45.
[76] Riggs BL, Melton LJ, Robb RA, Camp JJ, Atkinson EJ, McDaniel L, et al. A population-based assessment of rates of bone loss at multiple skeletal sites: evidence for substantial trabecular bone loss in young adult women and men. J Bone Miner Res 2008;23:205–14.
[77] Engelke K, Libanati C, Liu Y, Wang H, Austin M, Fuerst T, et al. Quantitative computed tomography (QCT) of the forearm using general purpose spiral whole-body CT scanners: accuracy, precision and comparison with dual-energy X-ray absorptiometry (DXA). Bone 2009;45:110–8.
[78] Zerfass P, Lowitz T, Museyko O, Bousson V, Laouisset L, Kalender WA, et al. An integrated segmentation and analysis approach for QCT of the knee to determine subchondral bone mineral density and texture. IEEE Trans Biomed Eng 2012;59:2449–58.
[79] Laval-Jeantet M, Laval-Jeantet AM, Lamarque JL, Demoulin B. An experimental study to evaluate mineralization of vertebral bone by computerized tomography (author's transl). J Radiol 1979;60:87–93.
[80] Laval-Jeantet AM, Roger B, Bouysee S, Bergot C, Mazess RB. Influence of vertebral fat content on quantitative CT density. Radiology 1986;159:463–6.
[81] Suzuki S, Yamamuro T, Okumura H, Yamamoto I. Quantitative computed tomography: comparative study using different scanners with two calibration phantoms. Br J Radiol 1991;64:1001–6.
[82] Bligh M, Bidaut L, White RA, Murphy WA, Stevens DM, Cody DD. Helical multidetector row quantitative computed tomography (QCT) precision. Acad Radiol 2009;16:150–9.
[83] Laval-Jeantet AM, Genant HK, Wu CY, Gluer CC, Faulkner KG, Steiger P. Factors influencing long-term in vivo reproducibility of QCT overtebral densitometry). J Comput Assist Tomogr 1993;17:915–21.
[84] Lian KC, Lang TF, Keyak JH, Modin GW, Rehman Q, Do L, et al. Differences in hip quantitative computed tomography (QCT) measurements of bone mineral density and bone strength between glucocorticoid-treated and glucocorticoid-naive postmenopausal women. Osteoporos Int 2005;16:642–50.
[85] Poole KE, Mayhew PM, Rose CM, Brown JK, Bearcroft PJ, Loveridge N, et al. Changing structure of the femoral neck across the adult female lifespan. J Bone Miner Res 2010;25:482–91.
[86] Bansal SC, Khandelwel N, Rai DV, Sen R, Bhadada SK, Sharma KA, et al. Comparison between the QCT and the DEXA scanners in the evaluation of BMD in the lumbar pine. J Clin Diagn Res 2011;5(4):694–9.
[87] Li N, Li XM, Xu L, Sun WJ, Cheng XG, Tian W. Comparison of QCT and DXA: osteoporosis detection rates in postmenopausal women. Int J Endocrinol 2013:5 [895474].
[88] Guglielmi G, Grimston SK, Fischer KC, Pacifici R. Osteoporosis: diagnosis with lateral and posteroanterior dual x-ray absorptiometry compared with quantitative CT. Radiology 1994;192:845–50.
[89] Forsen L, Sogaard AJ, Meyer HE, Edna T, Kopjar B. Survival after hip fracture: short- and long-term excess mortality according to age and gender. Osteoporos Int 1999;10:73–8.
[90] Szulc P, Munoz F, Marchand F, Delmas PD. Semiquantitative evaluation of prevalent vertebral deformities in men and their relationship with osteoporosis: the MINOS study. Osteoporos Int 2001;12:302–10.
[91] Engelke K, Kemmler W, Lauber D, Beeskow C, Pintag R, Kalender WA. Exercise maintains bone density at spine and hip EFOPS: a 3-year longitudinal study in early postmenopausal women. Osteoporos Int 2006;17:133–42.
[92] Looker AC, Wahner HW, Dunn WL, Calvo MS, Harris TB, Heyse SP, et al. Proximal femur bone mineral levels of US adults. Osteoporos Int 1995;5:389–409.
[93] Guglielmi G, Floriani I, Torri V, Li J, van Kuijk C, Genant HK, et al. Effect of spinal degenerative changes on volumetric bone mineral density of the central skeleton as measured by quantitative computed tomography. Acta Radiol 2005;46:269–75.
[94] Pacifici R, Rupich R, Griffin M, Chines A, Susman N, Avioli LV. Dual energy radiography versus quantitative computer tomography for the diagnosis of osteoporosis. J Clin Endocrinol Metab 1990;70:705–10.
[95] Genant HK, Engelke K, Fuerst T, Gluer CC, Grampp S, Harris ST, et al. Noninvasive assessment of bone mineral and structure: state of the art. J Bone Miner Res 1996;11:707–30.
[96] Eastell R, Mosekilde L, Hodgson SF, Riggs BL. Proportion of human vertebral body bone that is cancellous. J Bone Miner Res 1990;5:1237–41.
[97] Marshall LM, Lang TF, Lambert LC, Zmuda JM, Ensrud KE, Orwoll ES, et al. Dimensions and volumetric BMD of the proximal femur and their relation to age among older U.S. men. J Bone Miner Res 2006;21:1197–206.
[98] Genant HK, Cann CE, Ettinger B, Gordan GS. Quantitative computed tomography of vertebral spongiosa: a sensitive method for detecting early bone loss after oophorectomy. Ann Intern Med 1982;97:699–705.
[99] Nottestad SY, Baumel JJ, Kimmel DB, Recker RR, Heaney RP. The proportion of trabecular bone in human vertebrae. J Bone Miner Res 1987;2:221–9.
[100] Lang TF, Augat P, Lane NE, Genant HK. Trochanteric hip fracture: strong association with spinal trabecular bone mineral density measured with quantitative CT. Radiology 1998;209:525–30.
[101] Grampp S, Jergas M, Gluer CC, Lang P, Brastow P, Genant HK. Radiologic diagnosis of osteoporosis. Current methods and perspectives. Radiol Clin N Am 1993;31:1133–45.
[102] Min JK, Lin FY, Gidseg DS, Weinsaft JW, Berman DS, Shaw LJ, et al. Determinants of coronary calcium conversion among patients with a normal coronary calcium scan: what is the "warranty period" for remaining normal? J Am Coll Cardiol 2010;55:1110–7.

Please cite this article as: Mao SS, et al, Application of quantitative computed tomography for assessment of trabecular bone mineral density, microarchitecture and mechanica..., Clin Imaging (2015), http://dx.doi.org/10.1016/j.clinimag.2015.09.016

[103] Gourlay ML, Fine JP, Preisser JS, May RC, Li C, Lui LY, et al. Bone-density testing interval and transition to osteoporosis in older women. N Engl J Med 2012;366:225–33.
[104] Lenora J, Akesson K, Gerdhem P. Effect of precision on longitudinal follow-up of bone mineral density measurements in elderly women and men. J Clin Densitom 2010;13:407–12.
[105] Hillier TA, Stone KL, Bauer DC, Rizzo JH, Pedula KL, Cauley JA, et al. Evaluating the value of repeat bone mineral density measurement and prediction of fractures in older women: the study of osteoporotic fractures. Arch Intern Med 2007;167:155–60.
[106] Nelson HD, Haney EM, Dana T, Bougatsos C, Chou R. Screening for osteoporosis: an update for the U.S. Preventive Services Task Force. Ann Intern Med 2010;153:99–111.
[107] Lang TF, Li J, Harris ST, Genant HK. Assessment of vertebral bone mineral density using volumetric quantitative CT. J Comput Assist Tomogr 1999;23:130–7.
[108] Block JE, Smith R, Glueer CC, Steiger P, Ettinger B, Genant HK. Models of spinal trabecular bone loss as determined by quantitative computed tomography. J Bone Miner Res 1989;4:249–57.
[109] Gluer CC. Monitoring skeletal changes by radiological techniques. J Bone Miner Res 1999;14:1952–62.
[110] Naghavi M, Falk E, Hecht HS, Jamieson MJ, Kaul S, Berman D, et al. From vulnerable plaque to vulnerable patient–Part III: Executive summary of the Screening for Heart Attack Prevention and Education (SHAPE) Task Force report. Am J Cardiol 2006;98:2H–15H.
[111] Boutroy S, Bouxsein ML, Munoz F, Delmas PD. In vivo assessment of trabecular bone microarchitecture by high-resolution peripheral quantitative computed tomography. J Clin Endocrinol Metab 2005;90:6508–15.
[112] Khosla S, Riggs BL, Atkinson EJ, Oberg AL, McDaniel LJ, Holets M, et al. Effects of sex and age on bone microstructure at the ultradistal radius: a population-based noninvasive in vivo assessment. J Bone Miner Res 2006;21:124–31.
[113] Liu XS, Wang J, Zhou B, Stein E, Shi X, Adams M, et al. Fast trabecular bone strength predictions of HR-pQCT and individual trabeculae segmentation-based plate and rod finite element model discriminate postmenopausal vertebral fractures. J Bone Miner Res 2013;28:1666–78.
[114] Nishiyama KK, Pauchard Y, Nikkel LE, Iyer S, Zhang C, McMahon DJ, et al. Longitudinal HR-pQCT and image registration detects endocortical bone loss in kidney transplantation patients. J Bone Miner Res 2015;30:456–63.
[115] Parfitt AM, Drezner MK, Glorieux FH, Kanis JA, Malluche H, Meunier PJ, et al. Bone histomorphometry: standardization of nomenclature, symbols, and units. Report of the ASBMR Histomorphometry Nomenclature Committee. J Bone Miner Res 1987;2:595–610.
[116] Mueller TL, Stauber M, Kohler T, Eckstein F, Muller R, van Lenthe GH. Non-invasive bone competence analysis by high-resolution pQCT: an in vitro reproducibility study on structural and mechanical properties at the human radius. Bone 2009;44:364–71.
[117] Odgaard A, Gundersen HJ. Quantification of connectivity in cancellous bone, with special emphasis on 3-D reconstructions. Bone 1993;14:173–82.
[118] Kazakia GJ, Hyun B, Burghardt AJ, Krug R, Newitt DC, de Papp AE, et al. In vivo determination of bone structure in postmenopausal women: a comparison of HR-pQCT and high-field MR imaging. J Bone Miner Res 2008;23:463–74.
[119] Burghardt AJ, Kazakia GJ, Link TM, Majumdar S. Automated simulation of areal bone mineral density assessment in the distal radius from high-resolution peripheral quantitative computed tomography. Osteoporos Int 2009;20:2017–24.
[120] Meganck JA, Kozloff KM, Thornton MM, Broski SM, Goldstein SA. Beam hardening artifacts in micro-computed tomography scanning can be reduced by X-ray beam filtration and the resulting images can be used to accurately measure BMD. Bone 2009;45:1104–16.
[121] Nazarian A, Snyder BD, Zurakowski D, Muller R. Quantitative micro-computed tomography: a non-invasive method to assess equivalent bone mineral density. Bone 2008;43:302–11.
[122] Thurner PJ, Wyss P, Voide R, Stauber M, Stampanoni M, Sennhauser U, et al. Time-lapsed investigation of three-dimensional failure and damage accumulation in trabecular bone using synchrotron light. Bone 2006;39:289–99.
[123] Burghardt AJ, Kazakia GJ, Laib A, Majumdar S. Quantitative assessment of bone tissue mineralization with polychromatic micro-computed tomography. Calcif Tissue Int 2008;83:129–38.
[124] Kazakia GJ, Burghardt AJ, Cheung S, Majumdar S. Assessment of bone tissue mineralization by conventional x-ray microcomputed tomography: comparison with synchrotron radiation microcomputed tomography and ash measurements. Med Phys 2008;35:3170–9.
[125] Laib A, Newitt DC, Lu Y, Majumdar S. New model-independent measures of trabecular bone structure applied to in vivo high-resolution MR images. Osteoporos Int 2002;13:130–6.
[126] Yeni YN, Wu B, Huang L, Oravec D. Mechanical loading causes detectable changes in morphometric measures of trabecular structure in human cancellous bone. J Biomech Eng 2013;135:5 [54505].
[127] Gasser JA, Ingold P, Grosios K, Laib A, Hammerle S, Koller B. Noninvasive monitoring of changes in structural cancellous bone parameters with a novel prototype micro-CT. J Bone Miner Metab 2005;23:90–6 [Suppl.].
[128] Engelke K, Graeff W, Meiss L, Hahn M, Delling G. High spatial resolution imaging of bone mineral using computed microtomography. Comparison with microradiography and undecalcified histologic sections. Invest Radiol 1993;28:341–9.
[129] Boone JM, Velazquez O, Cherry SR. Small-animal X-ray dose from micro-CT. Mol Imaging 2004;3:149–58.
[130] Carlson SK, Classic KL, Bender CE, Russell SJ. Small animal absorbed radiation dose from serial micro-computed tomography imaging. Mol Imaging Biol 2007;9:78–82.
[131] Bredella MA, Misra M, Miller KK, Madisch I, Sarwar A, Cheung A, et al. Distal radius in adolescent girls with anorexia nervosa: trabecular structure analysis with high-resolution flat-panel volume CT. Radiology 2008;249:938–46.
[132] Issever AS, Link TM, Kentenich M, Rogalla P, Schwieger K, Huber MB, et al. Trabecular bone structure analysis in the osteoporotic spine using a clinical in vivo setup for 64-slice MDCT imaging: comparison to microCT imaging and microFE modeling. J Bone Miner Res 2009;24:1628–37.
[133] Ito M, Ikeda K, Nishiguchi M, Shindo H, Uetani M, Hosoi T, et al. Multi-detector row CT imaging of vertebral microstructure for evaluation of fracture risk. J Bone Miner Res 2005;20:1828–36.
[134] Diederichs G, Link TM, Kentenich M, Schwieger K, Huber MB, Burghardt AJ, et al. Assessment of trabecular bone structure of the calcaneus using multi-detector CT: correlation with microCT and biomechanical testing. Bone 2009;44:976–83.
[135] Diederichs G, Link T, Marie K, Huber M, Rogalla P, Burghardt A, et al. Feasibility of measuring trabecular bone structure of the proximal femur using 64-slice multidetector computed tomography in a clinical setting. Calcif Tissue Int 2008;83:332–41.
[136] Graeff C, Timm W, Nickelsen TN, Farrerons J, Marin F, Barker C, et al. Monitoring teriparatide-associated changes in vertebral microstructure by high-resolution CT in vivo: results from the EUROFORS study. J Bone Miner Res 2007;22:1426–33.
[137] Saha S, Roychowdhury A. Application of the finite element method in orthopedic implant design. J Long-Term Eff Med Implants 2009;19:55–82.
[138] Zysset PK, Dall'ara E, Varga P, Pahr DH. Finite element analysis for prediction of bone strength. BoneKEy Rep 2013;2:386.
[139] Liebl H, Garcia EG, Holzner F, Noel PB, Burgkart R, Rummeny EJ, et al. In-vivo assessment of femoral bone strength using Finite Element Analysis (FEA) based on routine MDCT imaging: a preliminary study on patients with vertebral fractures. PLoS One 2015;10:e0116907.
[140] Buckley JM, Loo K, Motherway J. Comparison of quantitative computed tomography-based measures in predicting vertebral compressive strength. Bone 2007;40:767–74.
[141] Keaveny TM, Hoffmann PF, Singh M, Palermo L, Bilezikian JP, Greenspan SL, et al. Femoral bone strength and its relation to cortical and trabecular changes after treatment with PTH, alendronate, and their combination as assessed by finite element analysis of quantitative CT scans. J Bone Miner Res 2008;23:1974–82.
[142] Chevalier Y, Quek E, Borah B, Gross G, Stewart J, Lang T, et al. Biomechanical effects of teriparatide in women with osteoporosis treated previously with alendronate and risedronate: results from quantitative computed tomography-based finite element analysis of the vertebral body. Bone 2010;46:41–8.
[143] Liu XS, Zhang XH, Sekhon KK, Adams MF, McMahon DJ, Bilezikian JP, et al. High-resolution peripheral quantitative computed tomography can assess microstructural and mechanical properties of human distal tibial bone. J Bone Miner Res 2010;25:746–56.
[144] Liu XS, Zhang XH, Rajapakse CS, Wald MJ, Magland J, Sekhon KK, et al. Accuracy of high-resolution in vivo micro magnetic resonance imaging for measurements of microstructural and mechanical properties of human distal tibial bone. J Bone Miner Res 2010;25:2039–50.
[145] Bauer JS, Sidorenko I, Mueller D, Baum T, Issever AS, Eckstein F, et al. Prediction of bone strength by muCT and MDCT-based finite-element-models: how much spatial resolution is needed? Eur J Radiol 2014;83:e36–42.
[146] Cody DD, Gross GJ, Hou FJ, Spencer HJ, Goldstein SA, Fyhrie DP. Femoral strength is better predicted by finite element models than QCT and DXA. J Biomech 1999;32:1013–20.
[147] Graeff C, Marin F, Petto H, Kayser O, Reisinger A, Pena J, et al. High resolution quantitative computed tomography-based assessment of trabecular microstructure and strength estimates by finite-element analysis of the spine, but not DXA, reflects vertebral fracture status in men with glucocorticoid-induced osteoporosis. Bone 2013;52:568–77.
[148] Amin S, Kopperdhal DL, Melton LJ, Achenbach SJ, Therneau TM, Riggs BL, et al. Association of hip strength estimates by finite-element analysis with fractures in women and men. J Bone Miner Res 2011;26:1593–600.
[149] Graeff C, Chevalier Y, Charlebois M, Varga P, Pahr D, Nickelsen TN, et al. Improvements in vertebral body strength under teriparatide treatment assessed in vivo by finite element analysis: results from the EUROFORS study. J Bone Miner Res 2009;24:1672–80.

Please cite this article as: Mao SS, et al, Application of quantitative computed tomography for assessment of trabecular bone mineral density, microarchitecture and mechanica..., Clin Imaging (2015), http://dx.doi.org/10.1016/j.clinimag.2015.09.016